Single particle cryo-EM structure elucidation of a Photosystem II complex mimicking a critical step in photoinhibition

Carolann Espy

X _____
Inga Schmidt-Krey

X _____
Raquel Lieberman

Table of Contents

Page

Abstract

Photosystem II (PSII) is an essential protein in the photosynthetic process that houses the oxygen evolution center, which is responsible for producing most of the oxygen in the atmosphere. In order to better understand PSII and its function, it is important to discern the structure of active PSII and the process of photoinhibition. Photoinhibition occurs when the extrinsic subunits are damaged due to overexposure to light, and are then removed, repaired, and replaced. The removal of these extrinsic subunits could be recreated with the help of a urea wash protocol, which removed subunits PsbO, PsbP, and PsbQ. The method used here to elucidate the structure of urea wash PSII, was electron cryo-microscopy (cryo-EM). Utilizing this method and a gentle purification of the protein, a 3D model of an important step in the repair of 'photoinhibited' PSII was obtained. Through testing multiple parameters during image processing, several models were generated with estimated resolutions ranging from 20.74 Å to the best estimated resolution of 9.05 Å (Figure 2).

Introduction

Photosynthesis is an important biochemical pathway in plants and other organisms to convert light energy into a usable form for these organisms such as adenosine triphosphate (ATP). There are many steps in this pathway including the light reactions and the Calvin cycle. The light reactions are the processes to convert light energy to chemical energy (ATP) and the Calvin cycle uses carbon dioxide and the ATP produced from the light reactions to make glucose. The light reactions occur within the thylakoid membrane and the two major proteins of this process are Photosystem I and Photosystem II. Photosystem II is the first protein in the light reaction schemes responsible for absorbing light and it also houses the oxygen evolving complex (OEC) (Enami 2008). The OEC is the center that is responsible for taking water and splitting it

into gaseous oxygen as well as electrons and protons, which transfer the energy from light and create a proton gradient, respectively. Photosystem II (PSII) is an integral protein in this photosynthetic process and therefore having knowledge of its structure is of the utmost importance due to its potential use in developing artificial solar energy convertors.

The structure of PSII has been previously studied using multiple methods including electron microscopy and x-ray diffraction (Wei et al. 2016, Suga et al. 2015); however, these structures did not represent active PSII. In addition, there is contradicting literature on the exact positionings of several subunits such as the three extrinsic subunits, PsbO, PsbQ, and PsbP. The activity of a protein depends in large part on maintaining the native structure of the protein, which can change based on alterations to the surrounding environment of the protein during and after its purification.

Electron cryo-microscopy (cryo-EM) is a method that can be used to image samples to obtain structural data at the angstrom level, and one major benefit is that it keeps the samples in a near native state (Cheng 2015). Therefore, it can help to maintain the activity of a protein sample of interest, which makes it an ideal method for the investigation of the structure of active PSII. By using this method and pairing it with a gentle purification method, the structure of active PSII may be achieved where previous EM PSII structures were not active.

With over 19 subunits, certain PSII subunits such as D1 and D2, which are the core subunits, have their functions and locations well characterized (Su et al. 2017, Wei et al. 2016). However, as outlined earlier the exact functions and positions have yet to be completely elucidated for many subunits. PsbO, PsbQ, and PsbP are three such subunits whose positioning are not clear (Suga et al. 2015, Umena et al. 2011). There is contradictory literature for the position of these three subunits. Certain literature proposes that the order of the three extrinsic

subunits going clockwise is PsbO, PsbP, and PsbQ, when viewed perpendicular to the plane of the membrane, and other literature proposes the reverse order of PsbQ, PsbP, and PsbO (Roose et al. 2016).

The main goal of this project was to compare both the three-dimensional structures and the amino acid sequences of the PSII subunits and core subunits. This helped with identifying the possible conformations of the extrinsic subunits of PSII and was then be applied to the three-dimensional structures previously obtained over the course of this project. Another major goal of this project was to identify the specific differences between the primary, secondary, and tertiary structures of PSII's extrinsic subunits of different species. This was be accomplished using structures and sequences previously determined in other experiments. By comparing these structures, differences in evolution of the structure and other information can help with the overall goal of the 3D optimization of PSII. Overall, PSII is responsible for nearly all primary energy sources in the world and is necessary for human life. Considering this information, it is essential to learn the structure of the protein to better understand its function in order to maximize crop growth as well as assist in the development of artificial solar energy convertors.

Literature Review

Photosystem II (PSII) is an integral membrane protein in the photosynthetic process of converting light, water, and carbon dioxide to oxygen and glucose. Found in the thylakoid membranes of chloroplasts, it directs electron transport and the creation of the proton gradient, which are used to produce the ATP required to form glucose. PSII is therefore responsible for nearly all primary energy sources in the world and is necessary for all life.

While the structure of inactive PSII is known, the structure of active PSII and the exact positions of some subunits is not. PSII has over 19 subunits. Although some of the functions of these subunits are known, such as D1 and D2, the core subunits of PSII, and PsbO, the manganese stabilizing protein, most of the subunits' functions and positions have yet to be completely elucidated (Su et al. 2017, Wei et al. 2016, Suga et al. 2015, Umena et al. 2011). PsbO, PsbQ, and PsbP are three such subunits whose positions are not clear. There is contradictory literature for the position of these three subunits. Some literature says the order is PsbO, PsbP, and PsbQ, and other literature says the order is PsbQ, PsbP, and PsbO (Roose et al. 2016).

A major goal of the project is to identify the correct positioning of these subunits, and this is done through the removal of subunits in different combinations (Boekema et al. 2000). PsbQ and PsbP may be removed using a salt wash, while PsbQ, PsbP, and PsbO may be removed using a urea wash (Halverson and Barry 2003). By imaging the three PSII types (active/control, urea wash, and salt wash) through single particle cryo-EM, the 3D models may be compared to understand the structure and locations of the subunits on PSII. An added bonus of removing the subunits from active PSII is that it allows for the investigation of the repair process of PSII. The repair process of PSII occurs after oxidative damage, typically to the core unit D1, from oxidizing water into gaseous oxygen (Theis and Schroda, 2016; Melis, 1999). The repair process begins by temporarily removing subunits PsbQ, PsbP, and PsbO, which is how the urea wash simulates this process, as it also removes the same subunits (Roose et al. 2016). The process ends with the core subunit being removed and replaced and the subunits reassociating with the complex. Understanding the repair process would allow us to help certain plants adapt to specific

stresses, which could in turn help increase the range of what would be considered farmable areas across the world.

As outlined earlier, single particle cryo-EM was used to image and then generate the 3D models of PSII. A significant benefit of single particle analysis is that the protein does not need to be crystallized, which is difficult in general and even more so for membrane proteins like PSII (Cheng 2015). Importantly, single particle cryo-EM allows for structural studies of somewhat heterogenous samples such as active PSII, where a certain degree of heterogeneity in terms of peripheral subunits is the cost of keeping the sample active. In single particle cryo-EM, the protein is flash-frozen in vitreous ice on a perforated TEM grid and imaged using an electron cryo-microscope. On the grid, the protein is suspended in a thin layer of vitreous ice in different orientations and typically these different orientations are selected using software (Scheres 2012). However, due to a certain degree of heterogeneity resulting from the gentle purification process required to obtain active PSII, the typical programs for automated particle selection result in a large number of particles that represent different sizes of PSII complexes, which leads to a poor 3D model. Therefore, specific particle sizes were picked manually in RELION and then exported to the software, cisTEM, to create class averages for each orientation of the protein (Li et al. 2013, Scheres 2012, Grant et al. 2018). These class averages are then compiled in three-dimensions to form the final 3D model of PSII.

In addition to studying PSII from spinach, which was chosen for its known inactive structure and ready availability, valuable insight may be gained from studying the structures and sequences of PSII from different species. Previous studies have shown that between PSII from different species, discrepancies exist not only in the structure of the extrinsic subunits, but also in the expression of these extrinsic subunits (Enami et al. 2008). For example, in cyanobacteria

instead of PsbP and PsbQ, PsbU and PsbV are present, which functionally act in primarily the same way (Nield and Barber 2006). PsbO is the center of the oxygen-evolving complex (OEC), which is responsible for the actual act of splitting water to prepare to release it as oxygen gas and is therefore present among PSII from most species (Nield et al. 2000). Observing the similarity of PsbO subunits of different species and comparing them with the differences between the other extrinsic subunits, will provide more information about the structures that can then be related to the protein activity. Resources such as the Protein Databank will be used in order to get the information regarding the structures and sequences of different species of PSII. After downloading the information, PyMOL can be used to isolate the extrinsic subunits for individual analysis. Then, the tertiary and secondary structures between the species may be compared and tabulated.

The current project, begun 2018, has involved extensive work with PSII and the image processing of electron cryo-microscopy (cryo-EM) data of samples with and without the three extrinsic subunits: PsbO, PsbP, and PsbQ (Boekema et al. 2000). Image processing programs such as RELION and cisTEM have been used in order to select the particles for analysis and then to process the images to produce a three-dimensional structure (Scheres 2012). This study continued this work to optimize the resolution of my current structures. In a final analysis, the structure analysis conducted will be combined for an understanding of the molecular basis for highly active plant PSII.

Methodology

Sample Preparation of Spinach PSII:

The first step is the isolation of PSII from market spinach and was performed by the Barry lab. It is purified using TX-100 detergent, differential centrifugation, OTG solubilization, and then treatment with PEG. This purification process is relatively delicate because it is the active protein that is being imaged and a more rigorous purification inactivates PSII.

Cryo-EM:

Single particle cryo-EM is the process used to image and then generate the 3D models of PSII. In single particle cryo-EM, the protein is vitrified on a grid and imaged using a cryo-EM. The cryo-EM images are collected at Florida State University on their FEI Titan Krios by Yusuf Uddin and Kasahun Neselu. On the grid, the protein is in different orientations and typically these different orientations are selected, "picked", using RELION software (Scheres 2012). However, due to the gentle purification process used here, the typical softwares pick too many particles that are different sizes of the PSII complex, which leads to a poor 3D model. Therefore, the particles are picked by hand and then exported to the software we use, cisTEM 1.0.0, to create class averages for each orientation of the protein (Li et al. 2013). These class averages are then compiled in three-dimensions to obtain the final 3D model of PSII.

This process was performed for the control PSII, the salt washed PSII, and the urea washed PSII. The final 3D models were compared to allow for conclusions to be reached about any changes in conformational state due to the removal of the extrinsic subunits.

Results

From the particle selection process performed in RELION, a total of 9192 particles for the Urea Wash PSII were manually picked. The particle size was on average 20 Å in length and 10 Å wide.

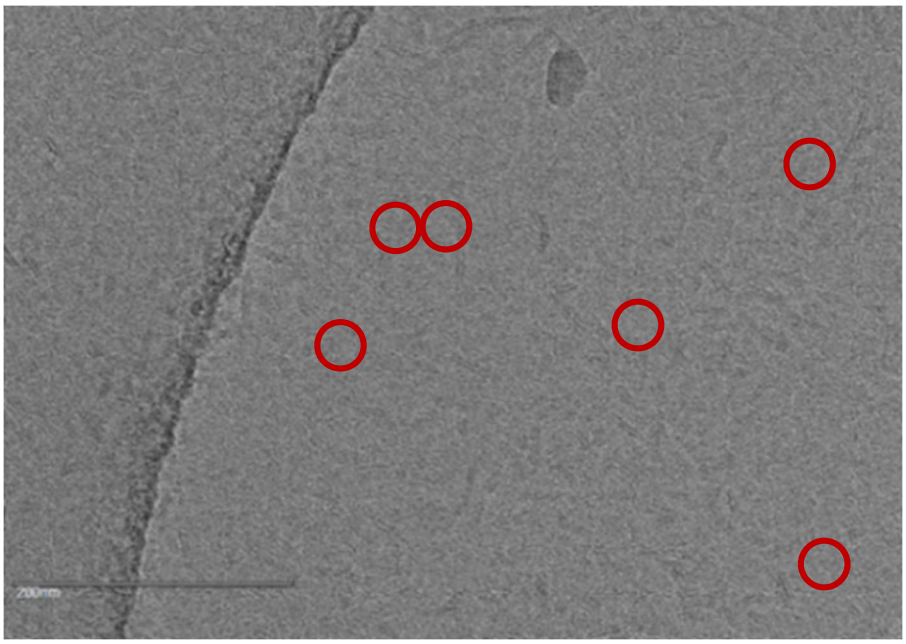

Figure 1. RELION image selection process. The micrograph above shows urea washed PSII particles (examples are circled in red). The scale bar corresponds to 200nm.

Table 1. Tested parameters and the resulting best estimated resolution when changing particle number, class averages, and cycles.

Particles	Class Averages	Cycles	Best Estimated Resolution
9192	150	20	17.37 Å
9192	100	20	17.37 Å
9192	50	50	17.37 Å

9192	30	50	17.37 Å
9192	20	50	17.37 Å
9192	25	50	16.48Å
8006	25	50	9.05Å

The total of 9192 particles in the urea wash sample were used to generate 3D structures from class averages of 150 and 100 run with 20 cycles as well as class averages of 50, 30, and 20 run with 50 cycles (Table 1). The class averages indicate the number of groups the particles were separated into based on similarity in the orientation and the cycles indicate how many times the particles were sorted. These 3D structures resulted in a resolution of 17.37 Å. The resolution could be increased to 9.05Å with a refinement package of 8006 particles and 25 class averages run through 50 cycles, which was most likely due to the removal of poor quality particles (Figure 2). Focus was then changed to adjusting the parameters for the global refinement step directly before the 3D model creation. A trend was observed that by using the 3D model from auto refinement as an initial model for the global refinement the signal to noise ratio is increased (Table 2). There also appeared to be regions with missing data in the final 3D model (Figure 3).

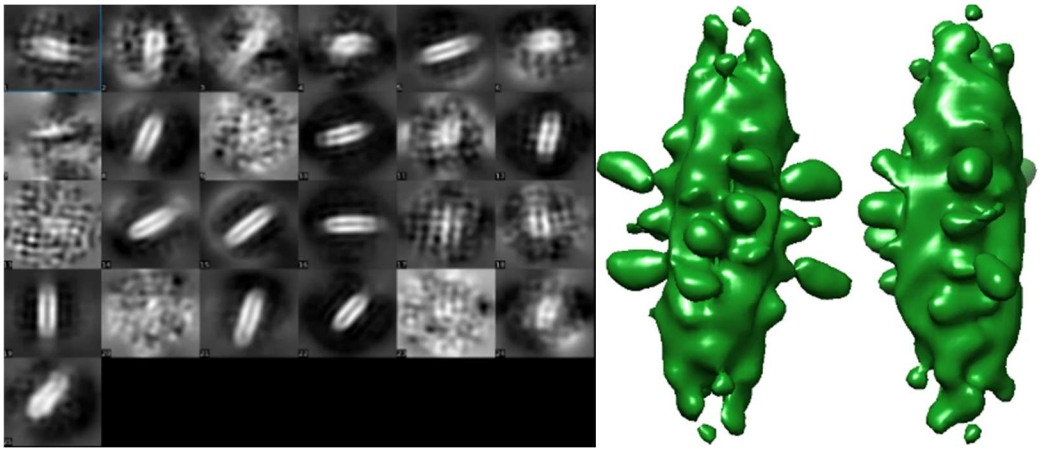

Figure 2. Left: Class averages of PSII. Twenty-five class averages were generated using 8006 urea washed PSII particles. Right: 3D model of Urea wash PSII. The 25 class averages were used to construct a cryo-EM density map at 9.05Å resolution.

Table 2. Best estimated resolution after auto refinement and then once that model was used as an input for global refinement. The cut off for the global auto and global input refinement was 30 Å.

Particles	Class Averages	Best Estimated Resolution after Auto Refinement	Best Estimated Resolution after Global Refinement
9192	10	20.74 Å	16.48 Å
9192	25	20.74 Å	19.48 Å
9192	50	14.94 Å	14.28 Å

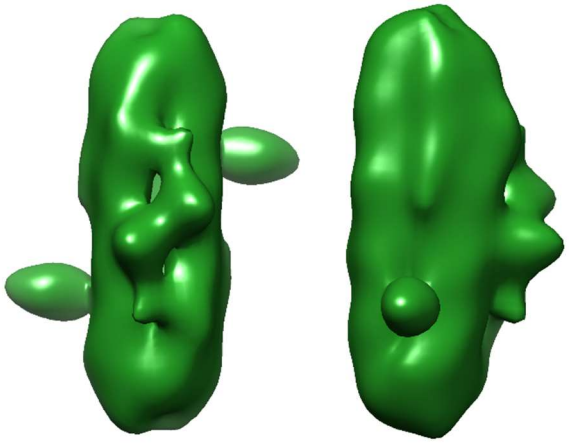

Figure 3. 3D model of Urea wash PSII from 9192 particles. The 50 class averages went through global refinement with random inputs and then used the output file as the input for a second run with a cut-off of 30Å resolution. The final resolution was found to be 14.28 Å.

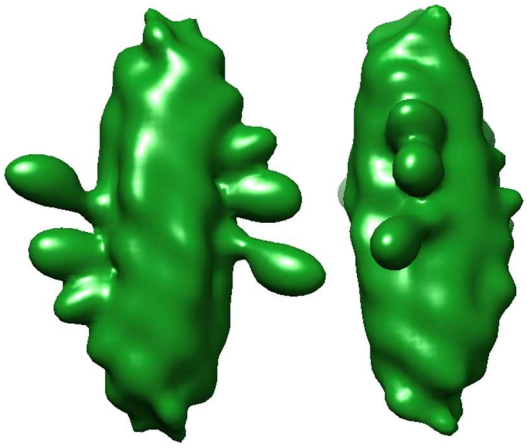

Figure 4. 3D model of Urea wash PSII from 9192 particles. The 25 class averages are used to construct a cryo-EM density map at 16.48Å resolution.

Discussion

The primary goal of this project was to obtain a structure of Photosystem II (PSII) at the highest resolution possible among the three different samples: control, salt-wash, and urea wash. Through optimizing the 3D model, a 9.05 Å resolution structure was produced from 8006 particles with 25 class averages run through 50 cycles (Figure 2). The improvement in resolution from the original model was partially due to the removal of over a thousand particles, which included poor images.

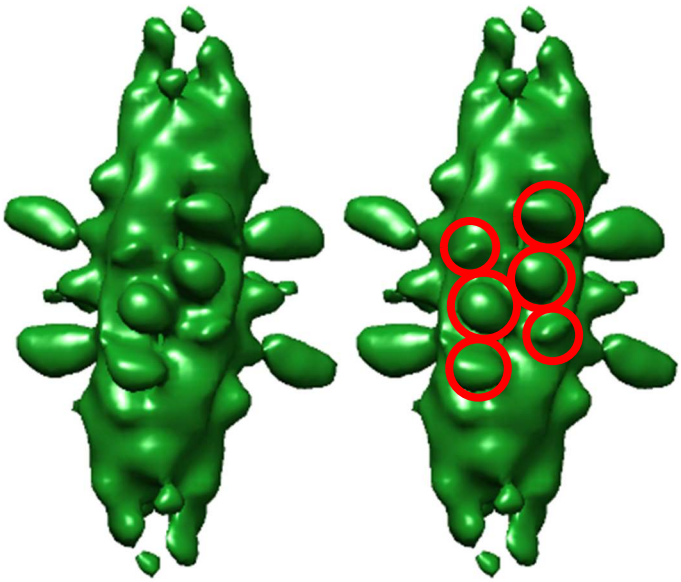

Figure 5. 9.05Å resolution structure next to the same structure with the extrinsic densities circled in red.

In the highest resolution model for the urea-wash PSII sample, densities that could corresponding to the three extrinsic subunits (PsbO, PsbP, and PsbQ) are visible. These densities, as seen circled in Figure 5, are in the positions that would be expected of the three extrinsic subunits. There are two main explanations for the presence of these densities: noise and ineffective urea wash. These densities could be due to noise at this contour level, so it cannot be said with certainty that they are due to the presence of the extrinsic subunits. However, if they are due to the extrinsic subunits, their presence would indicate that the urea wash was too gentle to force the extrinsic subunits to dissociate from the rest of the subunits for the majority of the sample. An important next step would be to compare this structure to an active PSII structure and see if the densities from the urea wash structure align with the extrinsic subunits on the active structure. There were 3D models generated that showed the lack of the extrinsic subunits, which shows that there was dissociation of the subunits for some of the sample; however, it may not have been at a high enough level to produce a structure on the 9 Å level as seen in Figure 2.

A 3D model that shows the lack of extrinsic can be seen in Figure 4. By using the full number of particle images (9192), a 16.48 Å resolution model was generated with 25 class averages run through 50 cycles. The appearance the extrinsic subunits after the removal of roughly a thousand images could indicate that the particles chosen during the refinement step were preferential towards those with the extrinsic subunits. The particles chosen had been selected due to quality of the images and in some cases the length of the images. Therefore, some of the lower quality images excluded from the 9.05 Å model may have been the particles without the extrinsic subunits.

Overall, a 3D model of urea wash Photosystem II with 9.05 Å resolution was produced from 8006 particles with 25 class averages run through 50 cycles. This was done after several hundred different iterations with varying parameters, and this was found to produce the highest resolution model. Through comparing the 3D models of the control and salt wash PSII samples prepared by fellow lab mates, Kasahun Neselu and Yusuf Uddin, slight differences between the samples were identified. The foremost difference was the length of the complexes. The control PSII was found to be slightly longer than the salt and urea wash samples, which was attributed to the light harvesting complex subunits still being attached to some of the control sample, but having been removed from the salt and urea wash. In the future, other computer programs such as EMAN 2.0 could be used to compare the 3D models generated to those generated by cisTEM 1.0.0. In addition, an automatic picker could potentially be used to select the particles from the obtained images in the future as well since there have been advancements in the selectivity of the programs.

Conclusion

Overall, a urea washed Photosystem II (PSII) structure was successfully obtained and the process optimized to provide the best structure at 9.05 Å resolution. Unfortunately, this structure showed the three extrinsic subunits PsbO, PsbP, and PsbQ, which could indicate that the urea wash was not strong enough to remove the subunits on all of the sample. An important next step will involve a comparison between the 9.05 Å resolution structure and the active control complex with the extrinsic subunits present, to compare the location of the densities observed in urea model to the intact complex. However, there are previous structures that show the sample without the extrinsic subunits even though it is at a worse resolution (16.48 Å). Therefore, some of the sample did successfully have the extrinsic subunits removed, but not enough to achieve a structure with better resolution. Automated particle picking with a reference that does not contain extrinsic subunits, may result in selection of particles that correspond to the reference and exclusion of particles that contain the extrinsic subunits. Additional, and even more critical future studies could include an increase in the urea concentration by a small amount in order to increase the ratio of PSII sample with the extrinsic subunits removed while maintaining the structure of the remainder of the protein. This last approach would have the significant benefit of obtaining the largest number of particles without the extrinsic subunits present, which would improve the signal-to-noise and the resulting resolution and quality of the model significantly, and thus allow for a detailed molecular understanding of the structure and repair process of PSII at the stage when all of the extrinsic subunits have been removed and are about to be replaced.

References

1. Boekema, E. J. van Breemen, J. F. L. van Roon, H. Dekker, J. P. Conformational Changes in Photosystem II Supercomplexes upon Removal of Extrinsic Subunits. *Biochemistry* 2000; 39 (42), 12907-12915.
2. Cheng, Y. Single-Particle Cryo-EM at Crystallographic Resolution. *Cell* 2015; 161(3): 450-457.
3. Enami, I. Okumura, A. Nagao, R. Suzuki, T. Iwai, M. Shen, J-R. Structures and functions of the extrinsic proteins of photosystem II from different species. *Photosynth Res* 2008; 98, 349-363.
4. Grant, T. Rohou, A. Grigorieff, N. cisTEM, user-friendly software for single-particle image processing. *eLife* 2018; 7: 35383.
5. Halverson, K.M. Barry, BA. Sucrose and Glycerol Effects on Photosystem II. *Biophysics Journal* 2003; 85(2): 1317–1325.
6. Li, X. Mooney, P. Zheng, S. Booth, C.R. Braunfeld, M.B. Gubbens, S. Agard, D.A. Cheng, Y. Electron counting and beam-induced motion correction enable near-atomic-resolution single-particle cryo-EM. *Nature Methods* 2013; 10: 584-590.
7. Melis, A. Photosystem-II damage and repair cycle in chloroplasts: what modulates the rate of photodamage in vivo? *Cell Press* 1999; 4(4): 130-135.
8. Nield, J. Barber, J. Refinement of the structural model for the Photosystem II supercomplex of higher plants. *BBA - Bioenergetics* 2006; 1757 (5-6), 353-361.
9. Nield, J. Kruse, O. Ruprecht, J. Fonseca, P. Buchel, C. Barber, J. Three-dimensional Structure of *Chlamydomonas reinhardtii* and *Synechococcus elongatu*s Photosystem II Complexes Allows for Comparison of Their Oxygen-evolving Complex Organization. *Journal of Biological chemistry* 2000. 275, 27940-27946.
10. Roose, J.L. Frankel, L.K. Mummadisetti, M.P. Bricker, T.M. The extrinsic proteins of photosystems II: update. *Planta* 2016; 243(4): 889-908.
11. Scheres, S.H.W. RELION: Implementation of a Bayesian approach to cryo-EM structure determination. *Journal of Structural Biology* 2012; 180(3): 519-530.
12. Su, X., Ma, J. Wei, X. Cao, P. Zhu, D. Chang, W. Liu, Z. Zhang, X. Li, M. Structure and assembly mechanism of plant C2S2M2-type PSII-LHCII supercomplex. *Science* 2017; 357 (6353), 815-820.
13. Suga, M. Akita, F. Hirata, K. Ueno, G. Murakami, H. Nakajima, Y. Shimizu, T. Yamashita, K. Yamamoto, M. Ago, H. Shen, J.R. Native structure of photosystem II at 1.95 A resolution viewed by femtosecond X-ray pulses. *Nature* 2015; 517: 99-103.
14. Theis, J. Schroda, M. Revisiting the photosystem II repair cycle. *Plant Signal Behavior* 2016; 11(9): e1218587.
15. Umena, Y. Kawakami, K. Shen, J.-R. Kamiya, N. Crystal structure of oxygen-evolving photosystem II at a resolution of 1.9A. *Nature* 2011; 473 (7345), 55-60.
16. Wei, X. Su, X. Cao, P. Liu, X. Chang, W. Li, M. Zhang, X. Liu, Z. Structure of spinach photosystem II–LHCII supercomplex at 3.2 Å resolution. *Nature* 2016; 534 (7605), 69-74.